Dealing With Link Blockage in mmWave Networks: A Combination of D2D Relaying, Multi-Beam Reflection, and Handover

Mingjie Feng, Shiwen Mao, *Fellow, IEEE*, and Tao Jiang, *Fellow, IEEE*

***Abstract*— In this paper, we consider adaptive user equipments (UE) link selection and user association in millimeter-wave (mmWave) networks. We formulate a joint optimization of link selection, resource allocation, and user association, aiming to maximize the sum logarithmic rate of all UEs. The formulated problem is solved by decomposing it into two levels of subproblems. The lower-level subproblem is link selection and resource allocation with a given user association, which is solved by a three-stage process. In the first stage, we establish the D2D relaying architecture by assuming that all UEs are served via D2D relaying. Based on the relaying architecture, we derive the optimal resource allocation in the second stage. Finally, an adaptive link selection algorithm is proposed in the third stage to determine the set of UEs that switch from D2D relaying to multi-beam reflection. The high-level subproblem is user association, for which we solve it with a dual decomposition-based approach. Simulation results indicate that compared to benchmark schemes, the average data rate achieved by the proposed scheme is significantly higher than the benchmark schemes and is close to an upper bound. Besides, the proposed scheme achieves a good tradeoff between system performance and fairness.**

***Index Terms*— 5G wireless, mmWave, D2D, multi-beam, link schedule, resource allocation, user association.**

I. Introduction

THE emergence of data-intensive mobile applications (e.g., ultra high definition video, augmented/virtual reality) has triggered a growing demand for high data rate services. To meet such demand, the fifth generation (5G) wireless network is designed to support the enhanced mobile broadband (eMBB) use cases by providing 1000x data rate [2]. Millimeter-wave (mmWave) communication is a key enabling technology of 5G wireless to achieve multi-Gbps data rate [3], [4]. Operating at the spectrum band ranging from 30 GHz to 300 GHz, a large bandwidth is available (e.g., a 850 MHz spectrum at 28 GHz band was approved by FCC for 5G), resulting in much higher data rate compared to traditional cellular networks. Due to such promising prospects, mmWave bands have been utilized in commercial 5G networks.

Despite such great potential, mmWave communication is challenged by its vulnerability to blockage. With short wavelength, mmWave signals can hardly penetrate obstacles such as human bodies and walls. As a result, the line-of-sight (LOS) path between a user equipment (UE) and a base station (BS) can be easily blocked as UEs move or change orientation [5]–[7]. When blockage happens, alternative links have to be established to restore connectivity. There are three possible approaches for link reestablishment, including (i) device-to-device (D2D) relaying between UEs, (ii) creating non-line-of-sight (NLOS) path with beam refection, (iii) handover to neighboring BSs. Dealing with blockage with one of the above approaches was considered in existing works. D2D-based mmWave communication was investigated in [8], [9], [11], [12], in which MAC protocols that support D2D relaying were designed. In [13], a multi-beam reflection framework was proposed to enable NLOS communication via reflection. In particular, the concept of beamspace MIMO was introduced and a multiplexing gain was achieved using multiple reflecting beams. The feasibility of establishing reliable NLOS links via reflection with commercial mmWave devices was verified in [35], and a beam switching mechanism was designed to quickly find the best alternative beam direction when blockage happens. The handover solution to blockage was also considered recently (e.g., in [14]–[16]). In [14], the BS-UE association was optimized based on inter-BS coordination. In [15], a machine learning-based solution was proposed for BSs to perform link blockage prediction, which enables proactive handover. In [16], an online machine learning framework was designed to capture the mobility and blockage patterns of users, which prevents unnecessary handover and reduces the signaling overhead.

Manuscript received 29 September 2021; revised 9 January 2022; accepted 14 February 2022. Date of publication 25 February 2022; date of current version 12 August 2022. This work was supported in part by NSF under Grant ECCS-1923717, in part by the National Science Foundation for Distinguished Young Scholars of China (NSFC) under Grant 61325004, and in part by NSFC under Grant 61771216. An earlier version of this paper was presented in part at the 28th Annual IEEE International Symposium on Personal, Indoor and Mobile Radio Communications (IEEE PIMRC 2017), Montreal, Canada, in October 2017 [DOI: 10.1109/PIMRC.2017.8292232]. The associate editor coordinating the review of this article and approving it for publication was D. Niyato. *(Corresponding author: Shiwen Mao.)*

Mingjie Feng is with the Wuhan National Laboratory for Optoelectronics, Huazhong University of Science and Technology, Wuhan 430074, China (e-mail: mzf0022@auburn.edu).

Shiwen Mao is with the Department of Electrical and Computer Engineering, Auburn University, Auburn, AL 36849 USA (e-mail: smao@ieee.org).

Tao Jiang is with the Wuhan National Laboratory for Optoelectronics and the School of Cyber Science and Engineering, Huazhong University of Science and Technology, Wuhan 430074, China (e-mail: tao.jiang@ieee.org).

Color versions of one or more figures in this article are available at https://doi.org/10.1109/TWC.2022.3152472.

Digital Object Identifier 10.1109/TWC.2022.3152472

Although the above approaches can effectively deal with blockage, the data rate performance is limited by certain inherent factors. For D2D relaying, a UE needs to share its communication resource with its relaying UEs. In addition, during multi-hop relaying, the UE data have to be forwarded multiple times, which increases the end-to-end delay. The major limiting factor of multi-beam reflection is the high path loss NLOS links. While the typical path loss exponent of LOS links is around 2, the path loss exponent of NLOS links can reach 4 [18]. Thus, only UEs under favorable conditions (e.g., close to BS or with good reflecting surfaces) can achieve satisfactory performance with multi-beam reflection. Moreover, as the BS transmission power is split among UEs, the power allocated to each UE would be small when the number of UEs is large, resulting in poor quality of service (QoS). The handover approach, which is easy to be implemented in sub-6 GHz cellular networks, requires intensive interaction between UEs and BSs as well as coordination between neighboring BSs. As narrow beams are used in mmWave communications, discovering alternative BSs and tracking roaming UEs incur considerable overhead in the control plane, such as that used for beam sweeping [17]. Besides, uncoordinated handover may cause imbalanced load distribution among BSs, resulting in resource underutilization. To fully harness the potential of these approaches in the presence of their limitations, a combination of multiple approaches with a proper integral design is highly appealing. This way, the number of UEs served by each approach decreased, resulting in more communication resources allocated to each UE. Under this context, how to properly select the set of UEs that utilizes each approach is a key design issue that determines the data rate performance, which has not been previously investigated. Given the nature of D2D relaying, multi-beam reflection, and handover, optimizing the use of these approaches is a two-step process. The first step is determining the set of UEs served by each BS, i.e., user association, which is *equivalent to* handover decisions. After user association is determined, the second step is selecting the proper link (D2D relaying or multi-beam reflection) for each NLOS UE.

In this paper, we consider a combination of D2D relaying, multi-beam reflection, and handover to deal with blockage in multi-cell mmWave networks [1]. We aim to improve the data rate performance as well as guarantee fairness among UEs with adaptive user association and link selection. The main contributions are summarized as follows.

- We formulate the joint optimization of link selection, resource allocation, and user association in mmWave networks as a mixed-integer linear programming (MILP) problem, aiming to maximize the sum logarithmic rate of all UEs.
- The formulated problem is decomposed into two levels of subproblems. The lower-level subproblem is link selection (between D2D relaying and multi-beam reflection) for each NLOS UE and resource allocation under a given user association. The higher-level subproblem is user association.
- The lower-level subproblem is solved with a three-stage process. In the first stage, we assume that all NLOS UEs are served by D2D relaying, and establish the D2D relaying architecture via a beam sweeping-based approach. Based on the relaying architecture, we derive the optimal resource allocation in the second stage. Given the resource allocation, a greedy algorithm is proposed for the link selection of each NLOS UE. The higher-level subproblem with a dual decomposition-based approach, which is implemented with iterative information exchange between UEs and BSs.
- The performance of the proposed solution is evaluated with simulations and compared with several benchmark schemes. The results show that, compared to the case with a single approach for dealing with blockage, a proper combination of multiple approaches can significantly improve the data rate performance. Besides, the proposed solution outperforms several heuristic schemes with considerable performance gain, and the performance is close to an upper bound. Moreover, fairness among UEs can be guaranteed, yielding a good tradeoff between system performance and fairness.

The rest of the paper is organized as follows. We first review related literature in Section II. The system model and problem formulation are introduced in Section III. We present the solution algorithm in Section IV. The simulation results are demonstrated and analyzed in Section V. Finally, we conclude this paper in Section VI.

II. Related Work

MmWave communications have drawn considerable attention in recent years. A fundamental analytical framework was introduced in [18]. In [19], urban measurements for the 28 GHz band were conducted, based on which a channel modeling framework and a capacity analysis were presented. The overviews of PHY layer and MAC layer techniques for mmWave communications can be found in [20] and [21], respectively. Compared to traditional wireless systems, a major feature of mmWave systems is that hybrid beamforming is used as a cost-effective approach to achieve both antenna gain and multiplexing gain [22], [23]. Another distinctive feature of mmWave communications is the need for beam sweeping during initial access. As narrow beams are used for directional communication, the transmitter and receiver need to scan multiple possible directions to discover each other and find the best Tx & Rx beam pair [24]–[26].

Dealing with blockage in mmWave communications with relaying has been considered in previous works. In [9], the effectiveness of D2D relaying in enhancing the coverage of mmWave cellular networks was analyzed based on a stochastic geometry framework. Under the context of multi-hop mmWave vehicular networks with fast varying environments, a deep reinforcement learning framework was proposed to optimize relay selection and power allocation [10]. In [11], D2D relaying was employed in mmWave small cell networks to support efficient multicasting, and a joint design of D2D path planning, transmission scheduling, and power control was proposed to improve the system energy efficiency. In the context of mmWave vehicular communications with vehicle-to-vehicle (V2V) relaying, a social-aware relay selection scheme was

proposed to fully harness the benefit of relaying in overcoming blockage [28]. Aiming to enhance the latency and reliability performance of mmWave multi-hop V2V communications, a relay selection design that considers channel characteristics, road topology, and traffic conditions was proposed [29]. From the perspective of network planning, the placement of relays was optimized to enhance the coverage of mmWave cells [30]. In [31], joint optimization of relaying selection and transmission scheduling was proposed to maximize the number of transmission flows in relay-assisted mmWave backhauls. In contrast to these works, we consider combining D2D relaying with the other two approaches to reduce the traffic load of each approach. Besides, we specify the process for establishing D2D relaying architecture, design the transmission pattern, and optimize the resource allocation to provide a comprehensive design for D2D relaying, aiming to fully exploit its potential.

Overcoming blockage with reflection was also studied in existing works. In [32], passive reflectors were employed to create NLOS links and improve the coverage of 28 GHz mmWave signals. Besides, the link qualities of NLOS paths generated by reflectors of different shapes, sizes, and materials were evaluated. In [33], tunable reflectors were used to augment vehicle to infrastructure (V2I) communications, and a deep reinforcement learning-based algorithm was developed for fast adjustment of reflector angle. From the perspective of network planning, the placement strategies of base stations and reflectors were optimized to maximize coverage as well as minimize the deployment cost [34]. Reflection-based alternative link establishment was implemented over commercial off-the-shelf (COTS) mmWave devices, and a real-time beam-switching algorithm was proposed for COTS devices to locate nearby reflectors and estimate their coefficients [35]. Recently, reconfigurable intelligent surface (RIS) based reflection was employed to overcome blockage in mmWave cellular systems. In [36], joint optimization of reflection coefficients and hybrid precoding/combining matrices was proposed to maximize the system spectral efficiency. Different from these works, we focus on the power allocation among UEs that utilize multi-beam reflection. Moreover, reflection is combined with other approaches for overcoming blockage, and we propose an adaptive selection scheme to fully utilize multiple approaches for performance improvement.

Handover and user association in mmWave systems have been widely investigated in the literature. To deal with the challenge of beam alignment caused by narrow beams in high mobility scenarios, a machine learning-based handover scheme was proposed in [37], which achieves fast handover by predicting the mobility of moving vehicles. To realize low-overhead handover, a multi-armed bandit framework was proposed to capture the user mobility and blockage pattern [38]. Recently, RIS was employed for efficient blockage-aware handover [39]. By optimizing the beamformers and RIS phase shifts, the impact of blockage can be mitigated, thus reducing the number of unnecessary handovers. In [40], user association was optimized to achieve a good tradeoff between spectrum efficiency and energy efficiency in mmWave backhaul small cell networks. In [41], load balancing-aware user association was investigated. Based on the features of mmWave links, user association was formulated as a mixed-integer nonlinear programming problem and solved with a polynomial-time algorithm. To avoid the high overhead of centralized control, a multi-agent reinforcement learning-based user association was proposed in [42], in which each UE acts as an agent and selects the associated BS based on its local observation, without having to carry out information exchange. In [43], user association and resource allocation were jointly optimized for a multi-band mmWave heterogeneous network, and an iterative framework was proposed to obtain a near-optimal solution. Our work differs from the above ones in that user association is used to determine the handover decision, and it is jointly optimized with link selection between D2D relaying and multi-beam reflection to achieve load balancing among BSs and better network-wide performance.

III. Problem Formulation

We consider a multi-cell mmWave network with J mmWave BSs indexed by $j \in \{1, \ldots, J\} \triangleq \mathcal{J}$, which collectively serve K UEs indexed by $k \in \{1, \ldots, K\} \triangleq \mathcal{K}$. The UEs are subject to random blockage. The UEs under blockage are served by the BSs via either D2D relaying or multi-beam reflection. The user association of UE k is indicated by the following binary variable[1]

$$x_{k,j} \triangleq \begin{cases} 1, & \text{if UE } k \text{ is associated with BS } j, \\ 0, & \text{otherwise.} \end{cases} \tag{1}$$

We consider the case that each UE can only associate with at most one BS, then $\sum_{j=1}^{J} x_{k,j} \leq 1, \forall k$. We also assume that the number of UEs associated with each BS j is upper bounded by U_j (e.g., U_j is the number of channels), then $\sum_{k=1}^{K} x_{k,j} \leq U_j, \forall j$. We consider all BSs operate in time division duplexing (TDD) mode, which enables efficient channel estimation via channel reciprocity. Since achieving high *downlink* data rates is the major objective for many data-intensive applications (e.g., VR/AR and UHD video), we focus on the design and optimization of downlink transmissions. The solution can be applied to the uplink transmissions with minor modifications. As shown in Fig. 1, we consider the downlink transmissions. Each NLOS UE has two options for establishing alternative links, a relaying UE or multi-beam reflection. Since there is no loop in the D2D relay, the relaying topology can be modeled as a tree with the BS being the root. Then, a multi-beam reflection link can be viewed as an alternative connection from the root to a node (i.e., an NLOS UE).

When UE k is served by BS j, the type of link utilized by UE k (i.e., multi-hop D2D relaying or multi-beam reflection) is indicated by two variables $\alpha_{k,j}$ and $\beta_{k,j}$, which are defined by

$$\alpha_{k,j} \triangleq \begin{cases} 1, \text{ UE } k \text{ utilizes D2D relaying or LOS link} \\ 0, \text{ otherwise,} \end{cases} \tag{2}$$

$$\beta_{k,j} \triangleq \begin{cases} 1, & \text{UE } k \text{ utilizes multi-beam reflection} \\ 0, & \text{otherwise,} \end{cases} \tag{3}$$

[1]When UE k is blocked, it is associated with BS j if it is connected to BS j via D2D relaying or multi-beam reflection.

TABLE I
SUMMARY OF RELATED WORK

Scenario \ Approach	Relaying		Reflection		Handover	
	Relay selection	Transmission scheduling	Reflector configuration	Beamforming	User association	Blockage analysis
Cellular network	[8], [9]		[36]	[13], [36]	[41]–[43]	[15], [38], [39]
V2X communication	[10], [28], [29]		[33]		[37]	
Backhaul	[31]	[31]			[40]	
Small cell network		[11], [12]			[40]	

TABLE II
SUMMARY OF NOTATIONS

Symbol	Definition
$x_{k,j}$	User association indicator of UE k
$\alpha_{k,j}$ and $\beta_{k,j}$	Link selection variables of UE k when served by BS j
$a_{k,k',j}$	Entry of descendent matrix of D2D relaying tree of BS j
$\rho_{k,j}$	Number of hops needed to transmit the packets of UE k
$\theta_{k,j}$	Number of transmissions that includes the packets of UE k in a downlink period
$t_{k,j}^{i,q}$	Fraction of time allocated to UE k on its ith hop during the qth transmission
$C_{k,j}^{i}$	Link capacity of the ith hop of UE k when served by BS j
$\gamma_{k,j}^{i}$	SINR of the ith hop link of UE k when served by BS j.
$h_{k,j}^{i}$, $G_{k,j}^{i}$, $d_{k,j}^{i}$, $p_{k,j}^{i}$	Small-scale fading factor, antenna gain, propagation distance, and transmission power of the ith hop transmission of UE k, respectively.
$h_{k,j}^{m}$, $\tilde{p}_{k,j}^{m}$, $G_{k,j}^{m}$, $d_{k,j}^{m}$	Small-scale fading factor, power, antenna array gain, and distance of the mth path, respectively.
$\tilde{p}_{k,j}$	Transmission power allocated to UE k when served by BS j via multi-beam reflection
$N_{\mathrm{LOS},j}$	Number of LOS UEs served by BS j
$M_{k,j}$	Number of reflecting beams serving UE k
$R_{k,j}$ and $\tilde{R}_{k,j}$	Data rate of UE k when served by BS j via D2D relaying and multi-beam reflection, respectively.
N_{BS} and N_{UE}	Number of directions to be swept by the BS and the UE during beam sweeping, respectively.
$\Delta_{k,j}^{[\tau]}$	Performance gain of all UEs when UE k switches from D2D relaying to multi-beam reflection at the τth round of Algorithm 1

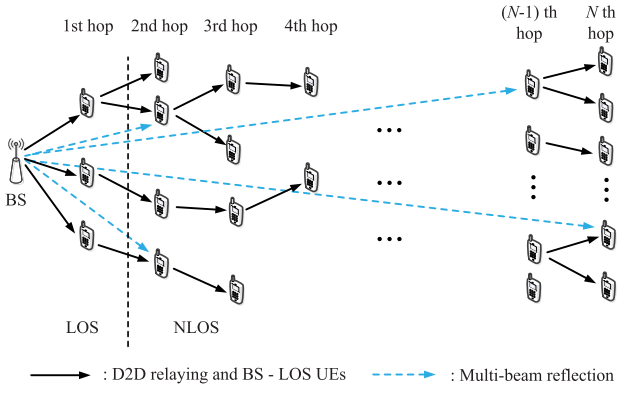

Fig. 1. Downlink transmissions of an mmWave cellular network supported by D2D relaying and multi-beam reflection.

Based on the definitions from (1) to (3), we have $\alpha_{k,j}+\beta_{k,j} = x_{k,j}$ for $k \in \mathcal{K}, j \in \mathcal{J}$. Note that we have $\alpha_{k,j} = 1$ for all LOS UEs since they are part of the D2D relaying architecture. Since $\alpha_{k,j} \leq x_{k,j}$ and $\sum_{k=1}^{K} x_{k,j} \leq U_j$, we have $\sum \alpha_{k,j} \leq U_j$. Similarly, we have $\sum \beta_{k,j} \leq U_j$. For UEs served by BS j with $\alpha_{k,j} = 1$, their relaying routes are indicated by a *descendent matrix*, in which the entries are defined by

$$a_{k,k',j} \triangleq \begin{cases} 1, & \text{UE } k' \text{ is a descendent of UE } k \\ 0, & \text{otherwise,} \end{cases} \tag{4}$$

Since $\{a_{k,k',j}\}$ are defined for UEs that are involved in D2D relaying, we have $a_{k,k',j} \leq \alpha_{k,j}$ and $a_{k,k',j} \leq \alpha_{k',j}$ for $k \in \mathcal{K}, j \in \mathcal{J}$. Denote $\rho_{k,j}$ as the depth of UE k in the D2D relaying tree, given by

$$\rho_{k,j} = \sum\nolimits_{k' \neq k} a_{k',k,j} + 1. \tag{5}$$

It can be seen that $\rho_{k,j}$ is the number of hops required to transmit the packets of UE k. Let N be the maximum value of $\rho_{k,j}$, which is the largest number of hops that can be supported by the network.[2] As shown in Fig. 2, to accommodate N hops of relaying, we divide the downlink transmission period into N time slots, indexed by $i = 1, \ldots, N$. The ith time slot is

[2]Theoretically, the maximum number of hops for each route should be different, since it is impacted by channel quality between UEs and the maximum latency. In our problem, all relaying transmissions must be completed within the downlink period of a TDD frame, and each time slot a downlink period is used to transmit one hop of user packets. Thus, the maximum allowable number of hops that can be supported is determined by the number of time slots in a downlink period, which is the same for all routes.

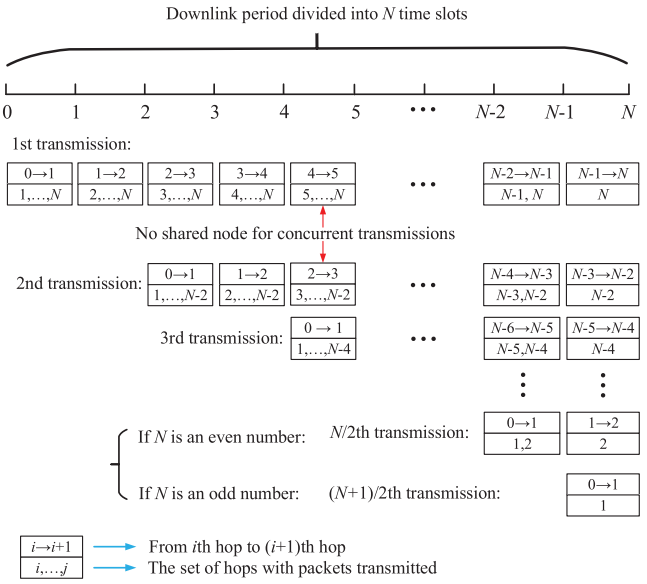

Fig. 2. Transmission pattern of a TDD-based multi-hop D2D mmWave cellular network.

used to transmit packets from the ith-hop UEs (i.e., UEs with $\rho_{k,j} = i$) to the $(i+1)$th-hop UEs (i.e., UEs with $\rho_{k,j} = i+1$). This way, the packets of the Nth-hop UEs can be received at the end of the downlink period. For UEs that are connected to the BS via multi-beam reflection, the entire downlink period is utilized for data transmission.

We assume that all UEs can only support half duplex communication. Thus, adjacent links (i.e., those share the same UE as Tx/Rx) cannot be utilized for data transmission concurrently [27]. Given this constraint, the total number of transmissions that can be implemented during a downlink period is $\lceil \frac{N}{2} \rceil$. The transmission pattern is as shown in Fig. 2. The packets of each UE are sent with multiple rounds of transmissions, each consisting of multiple stages. For example, after the 2nd stage of the 1st transmission (from 1st-hop UEs to 2nd-hop UEs) is completed, the 2nd transmission can be initiated, since the 1st-hop UEs have completed their transmissions and are free for reception. As the transmissions continue and the index of transmissions increases, the packets of UEs with larger $\rho_{k,j}$ are not transmitted, since there is not enough time to complete these transmissions. Specifically, the packets of UEs with $\rho_{k,j} = N-1$ and $\rho_{k,j} = N$ are not included in the 2nd transmission; the packets of UEs with $\rho_{k,j} = N-3, \ldots, N$ are not included in the 3rd transmission, and so on. Let $\theta_{k,j}$ be the number of transmissions that include the packets of UE k, it is calculated by

$$\theta_{k,j} = \begin{cases} \dfrac{N}{2} - \left\lceil \dfrac{\rho_{k,j}}{2} \right\rceil + 1, & N \text{ is even} \\ \dfrac{N+1}{2} - \left\lfloor \dfrac{\rho_{k,j}}{2} \right\rfloor, & N \text{ is odd,} \end{cases} \tag{6}$$

With advanced spatial multiplexing techniques, such as hybrid beamforming [23], an mmWave BS is can serve multiple UEs using the same time-frequency resource block. In contrast, due to hardware constraints, when a UE relays the packets of multiple UEs, orthogonal time-frequency resource has to be allocated to these UEs. Without loss of generality, we consider time division multiple access (TDMA) is applied when a UE forwards the packets of multiple UEs to the next-hop UE. Specifically, a fraction of time in each time slot is exclusively allocated to transmit the data of each UE. Denote $t_{k,j}^{i,q}$ as the fraction of time allocated to UE k on its ith hop during the qth transmission. Consider the outflow of a relaying UE, $t_{k,j}^{i,q}$ should satisfy

$$\sum_{k' \neq k} a_{k,k',j} t_{k',j}^{\rho_{k,j}+1,q} \leq 1, \quad k \in \{k \,|\rho_{k,j} \leq N-1\}, \\ q = 1, \ldots, \theta_{k,j} + \left\lceil \frac{\rho_{k,j}}{2} \right\rceil. \tag{7}$$

For UEs with $\rho_{k,j} = 1$, i.e., the LOS UEs, the inflow constraint is given by

$$\sum_{k' \neq k} a_{k,k',j} t_{k',j}^{1,q} + t_{k,j}^{1,q} \leq 1, k \in \{k \,|\rho_{k,j} = 1\}, \\ q = 1, \ldots, \left\lceil \frac{N}{2} \right\rceil. \tag{8}$$

The inflow constraint (8) only applies to the 1st-hop transmission. This is because the inflow packets received by other hops ($\rho_{k,j} > 1$) are sent within a fraction of a time slot due to the TDMA-based allocation at the previous hop. As each relaying UE only receives packets from one UE (see the D2D relaying tree shown in Fig. 1), the duration of packet reception is always shorter than or equal to that of a time slot. Thus, for UEs with $\rho_{k,j} > 1$, the left-hand side of (8) is always no larger than 1. Besides outflow and inflow constraints, $\{t_{k,j}^{i,q}\}$ also follows constraints result from the data rates of neighboring links. Specifically, the data rate of the link between the previous hop and the current hop should be no less than the data rate of the link between the current hop and the next hop. Thus, $\{t_{k,j}^{i,q}\}$ should also satisfy

$$C_{k,j}^{i} t_{k,j}^{i,q} \geq C_{k,j}^{i+1} t_{k,j}^{i+1,q}, \\ k \in \{k \,|\rho_{k,j} \geq 2\}, \quad i = 1, \ldots, \rho_{k,j} - 1, \tag{9}$$

where $C_{k,j}^{i}$ is the link capacity of the ith hop of UE k when served by BS j, given by

$$C_{k,j}^{i} = B \log\left(1 + \gamma_{k,j}^{i}\right), \tag{10}$$

where B is the system bandwidth and $\gamma_{k,j}^{i}$ is the SINR of the link for the ith hop of UE k when served by BS j. Note that, we assume that $\gamma_{k,j}^{i}$ remains a constraint over all the $\theta_{k,j}$ transmissions, since the downlink period is shorter than the coherence time of a TDD system.

Based on the SINR model presented in [18], we derive the SINR expressions for different types of links. When UE k is served by D2D relaying, the SINR is given by

$$\gamma_{k,j}^{i} = \frac{1}{\sigma^2} p_{k,j}^{i} h_{k,j}^{i} G_{k,j}^{i} (d_{k,j}^{i})^{-2}, \tag{11}$$

where $h_{k,j}^{i}$ is the small scale fading factor, which is a normalized Gamma random variable [18]; $G_{k,j}^{i}$ is antenna array gain; $d_{k,j}^{i}$ and $p_{k,j}^{i}$ are the propagation distance and transmission power for the ith hop transmission of UE k,

respectively. The noise power is σ^2. Due to the "pseudo-wired" property and large propagation loss of mmWave communications, we neglect the impact of interference in the SINR model. Since each D2D transmission is under an LOS link, the path loss exponent is set to be 2 according to [18].

We assume that the transmission power of BS j is equally allocated to UEs served by BS j with multi-beam reflection and LOS UEs. Hence, the transmission power allocated to each UE is given by

$$\tilde{p}_{k,j} = \frac{P_j}{\sum_k \beta_{k,j} + N_{\mathrm{LOS},j}}, \tag{12}$$

where P_j is the transmission power of BS j, $N_{\mathrm{LOS},j}$ is the number of LOS UEs served by BS j. Similar to (11), the SINR UE k when served with an LOS link is given by

$$\gamma^1_{k,j} = \frac{1}{\sigma^2}\tilde{p}_{k,j} h^1_{k,j} G^1_{k,j} (d^1_{k,j})^{-2}. \tag{13}$$

Suppose UE k is served by a total number of $M_{k,j}$ reflecting beams, indexed by $m = 1, \ldots, M_{k,j}$. Let $\tilde{\gamma}^m_{k,j}$ be the SINR of the mth beam of UE k, it is calculated by

$$\tilde{\gamma}^m_{k,j} = \frac{1}{\sigma^2}\tilde{p}^m_{k,j} h^m_{k,j} G^m_{k,j} (d^m_{k,j})^{-4}, \tag{14}$$

where $h^m_{k,j}$, $\tilde{p}^m_{k,j}$, $G^m_{k,j}$, and $d^m_{k,j}$ are the small-scale fading factor, transmission power, antenna array gain, and distance of the mth path, respectively. The interference caused by side lobes is negelected. The path loss factor of all NLOS reflecting links is 4. Without loss of generality, we assume $\tilde{p}_{k,j}$ is equally allocated to the $M_{k,j}$ beams.

Given the SINR expressions, the data rate of UEs under different links can be derived. When UE k is served by BS j with D2D relaying, its data rate is the sum of all the $\theta_{k,j}$ transmissions. For each transmission, the actual data rate is the data rate of the *final hop* divided by the number of hops. Then, the data rate of UE k when served by BS j via D2D relaying is given by

$$R_{k,j} = \sum_{j=1}^{\theta_{k,j}} \frac{1}{\rho_{k,j}} C^{\rho_{k,j}}_{k,j} t^{\rho_{k,j},q}_{k,j}. \tag{15}$$

The data rate of the LOS UEs is a special case of (15) when $\rho_{k,j} = 1$.

For UEs k served by multi-beam reflection, their data rate is the sum of data rates of all beams, which is given by

$$\tilde{R}_{k,j} = \sum_{m=1}^{M_{k,j}} B \log\left(1 + \tilde{\gamma}^m_{k,j}\right). \tag{16}$$

In this paper, we aim to maximize the sum logarithm rate of all UEs with joint optimization of link selection, resource allocation, and user association.[3] Let $\mathbf{x}$, $\boldsymbol{\alpha}$, $\boldsymbol{\beta}$, $\mathbf{a}$, and $\mathbf{t}$ be the vector/matrix forms of $\{x_{k,j}\}$, $\{\alpha_{k,j}\}$, $\{\beta_{k,j}\}$, $\{a_{k,k',j}\}$, and $\{t^{i,q}_{k,j}\}$. The problem is formulated as

$$\mathbf{P1:} \quad \max_{\{\mathbf{x},\boldsymbol{\alpha},\boldsymbol{\beta},\mathbf{a},\mathbf{t}\}} \sum_{k=1}^{K}\sum_{j=1}^{J} x_{k,j}\left\{\alpha_{k,j}\log R_{k,j} + \beta_{k,j}\log \tilde{R}_{k,j}\right\}$$

subject to: $(7) - (9)$

$$\sum\nolimits_{j=1}^{J} x_{k,j} \le 1, \quad k \in \mathcal{K}, \tag{17}$$

$$\sum\nolimits_{k=1}^{K} x_{k,j} \le U_j, \quad j \in \mathcal{J}, \tag{18}$$

$$\alpha_{k,j} + \beta_{k,j} = x_{k,j}, \quad k \in \mathcal{K},\ j \in \mathcal{J}, \tag{19}$$

$$\sum\nolimits_{k' \ne k} a_{k',k,j} \le 1,\ k \in \{k \,|\rho_{k,j} \le 2\}, \tag{20}$$

$$a_{k,k',j} \le \alpha_{k,j},\ k \in \mathcal{K}, \tag{21}$$

$$0 \le t^{i,q}_{k,j} \le \alpha_{k,j},\ k \in \mathcal{K}, j \in \mathcal{J}, \quad i = 1, \ldots, N, q = 1, \ldots, \theta_{k,j}, \tag{22}$$

$$x_{k,j}, \alpha_{k,j}, \beta_{k,j}, a_{k,k',j} \in \{0,1\}, \quad k \in \mathcal{K}, j \in \mathcal{J}. \tag{23}$$

Constraint (20) results from the fact that each node can only have at most one parent node in the D2D relaying tree. All other constraints have been explained before in this section.

IV. Solution Algorithm

Problem **P1** is a mixed-integer programming problem with multiple sets of coupled variables. Solving it with standard techniques incurs prohibitive complexity. Therefore, we decompose Problem **P1** into two levels of subproblems. The lower-level is link selection and resource allocation with a given user association, and we solve it with a three-stage process. The higher-level is user association given that the solution of the lower-level subproblem will be applied, which is solved by a dual decomposition-based algorithm.

The reasons for decomposing Problem **P1** with the above pattern are as follows. First, as mentioned in the previous section, link selection and resource allocation are optimized based on the outcome of user association. Due to this fact, $\{\alpha_{k,j}\}$, $\{\beta_{k,j}\}$, and $\{t^{i,q}_{k,j}\}$ are defined based on $\{x_{k,j}\}$. Second, link selection and resource allocation are mutually coupled. Specifically, resource allocation is optimized for the set of UEs that are served by D2D links, which are determined by the link selection strategy; the link selection of UEs is based on the data rates of D2D and multi-beam reflection links, which depend on the outcome of resource allocation. Third, user association is determined by the achievable data rates of UEs when connecting to different BSs, which is impacted by link selection and resource allocation. Other ways of decomposing Problem **P1**, such as optimizing link selection and user association under given resource allocation (higher-level subproblem) and resource allocation (higher-level subproblem), are not reasonable. For example, link selection would be meaningless for a UE unless its associated BS has been confirmed, and resource allocation among D2D UEs cannot be performed before link selection is determined. Therefore, we set user association as the higher-level subproblem and set link selection and resource allocation under given user association as the lower-level subproblem.

[3]We consider joint optimization of link selection, resource allocation, and user association since these strategies are coupled. For example, user association directly determines the traffic load of each BS and the achievable data rate of each UE when selecting different links, which impact the link selection strategy. Thus, instead of solving each problem separately, we formulate and solve the joint optimization of the three strategies.

A. Link Selection and Resource Allocation With Given User Association

With a given user association, the link selection and resource allocation are determined by a three-stage process. In the first stage, we set all UEs associated with a BS to be served with D2D relaying, and establish the D2D relaying architecture (i.e., $\{a_{k,k',j}\}$) with a beam sweeping-based approach. In the second stage, we derive the optimal resource allocation under the derived D2D relaying architecture. In the third stage, based on the outcome of resource allocation, we evaluate the data rate gains achieved by UEs when they switch from D2D relaying to multi-beam reflection, and accordingly determine the set of UEs to be served by multi-beam reflection.

As user association is given, UEs served by different BSs are independent of each other. Thus, problem **P1** can be decomposed into J independent problems, each corresponds to the sum logarithm rate maximization of UEs served by the same BS. Without loss of generality, we consider the link selection and resource allocation of BS j.

1) D2D Relaying Architecture Establishment: To establish the D2D relaying architecture, the neighboring UEs need to discover each other and estimate the link qualities between them. Due to the directionality of mmWave communication, *beam sweeping* is required for UEs to find the best Tx & Rx beam directions between them. After beam sweeping is completed, each receiving UE identifies the best Tx/Rx beam pairs (e.g., the Tx/Rx beam direction with the highest received power) between itself and various potential relaying UEs, and records the link qualities under the best beam pairs. Then, each UE selects the UE with the best link quality as its relaying UE (i.e., parent node in the D2D relaying tree). The D2D relaying architecture is established after all NLOS UEs have selected their relaying UEs.

The detailed process of beam sweeping is described as follows. As we assume that all UEs can only perform half-duplex communication, beam sweeping has to be performed sequentially between BS and LOS UEs and between neighboring hops of UEs, which is similar to the transmission pattern shown in Fig. 2. Recall that the maximum number of hops for D2D relaying is N. To support N hops of relaying, the D2D relaying architecture must be sequentially established in N steps. To this end, we divide the period for D2D relaying architecture establishment into N time slots, indexed by $i = 1, \ldots, N$. The first time slot is used for beam sweeping between the BS and UEs at the first hop (i.e., LOS UEs), and the ith time slot ($i > 1$) is used for the beam sweeping and relay selection between UEs at the ith hop and UEs at the $(i+1)$th hop. Since the D2D relaying architecture is based on LOS links, only LOS signals are evaluated during beam sweeping, which can be identified via existing approaches [45]. By identifying LOS signals, each UE obtains its value of $\rho_{k,j}$ (i.e., the number of hops needed to communicate with the BS). Specifically, the UEs that can receive LOS signals from the BS are first-hop UEs (i.e., LOS UEs), the UEs that can receive LOS signals from first-hop UEs are second-hop UEs, the UEs that can receive LOS signals from second-hop UEs are third-hop UEs, and so on. Considering that the UEs have no prior knowledge about their values of $\rho_{k,j}$, each UE needs to perform Rx beam sweeping (i.e., receive with different beam directions) until it has selected its relaying UE. Specifically, the LOS UEs will perform one round of Rx beam sweeping in the first time slot, the 2nd-hop UEs will perform two rounds of Rx beam sweeping in the first and second time slots, the ith hop UEs will perform i rounds of Rx beam sweeping from the first time slot to the ith time slot, and so on.

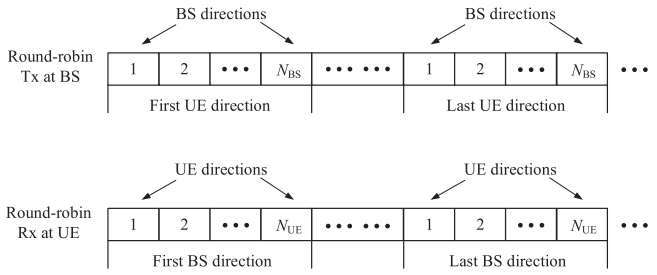

Fig. 3. Beam sweeping process between BS and UE.

The beam sweeping between the BS and LOS UEs is performed by the BS sequentially sending multiple predefined signals (e.g., synchronization signal blocks in NR) along with different Tx beam directions. At the UE side, all UEs receive the *LOS components* of these signals with different Rx beam directions, and record the link qualities of all Tx/Rx beam pairs. Let N_{BS} and N_{UE} be the number of directions to be swept by the BS and the UE, respectively. The beam sweeping can be performed in two ways. The first way is shown in the upper part of Fig. 3, where the BS sequentially sends N_{BS} copies of signals along with all the N_{BS} directions in a round-robin fashion, and this process is repeated for N_{UE} rounds. Within each round, the UE receives a set of N_{BS} signals with one of the N_{UE} directions; when the next round begins, the UE switch to the next direction to receive another set of N_{BS} signals. The second way is shown in the lower part of Fig. 3, where the BS repeatedly sends N_{UE} copies of signals along with one of the N_{BS} directions; after that, it sends N_{UE} copies of signals along the next direction. This process is repeated for all the N_{BS} Tx directions. At the UE side, the UE sequentially receives a complete round of N_{UE} signals with all the N_{UE} directions in a round-robin fashion, and repeat this process until all the N_{BS} rounds of signal reception are completed.

After the beam sweeping between BS and 1st-hop UE (i.e., LOS UE) is completed, the beam sweeping between 1st-hop and 2nd-hop UEs is performed in the second time slot. Similarly, the 1st-hop UEs sequentially send predefined signals along with different Tx directions; then the remaining UEs receive the LOS components of these signals with different Rx directions, and record the link qualities of all Tx/Rx beam pairs. The UEs that have received LOS signals from 1st-hop UEs identify themselves as the 2nd-hop UEs, and initiate the beam sweeping in the third time slot by sending predefined signals along with different directions. The remaining UEs (other than 1st-hop and 2nd-hop UEs) receive the LOS components of these signals and record the best beam pairs; the UEs that have received LOS signals from 2nd-hop UEs identify themselves as the 3rd-hop UEs, and initiate the next

round of beam sweeping. The above process continues until the Nth-hop UEs have completed their LOS signal reception and recorded the best beam pair.

To enable the Rx UEs to record the link qualities of various Tx UEs, the signals used for beam sweeping between UEs are designed to carry the ID of Tx UEs. Along with ID, the Tx UEs also attach their selections of relaying UE in the beam sweeping signals. As all the relaying UEs share their UE selections to their next-hop UEs, the routing path of each UE can be obtained by aggregating the selections of the UEs at its previous hops, which finalizes the process for D2D relaying architecture establishment. After the relaying architecture is established, each NLOS UE sends its uplink data and relaying path information to the BS via the obtained D2D path.

2) Optimal Resource Allocation Under D2D Relaying: With the D2D relaying architecture, the resource allocation of BS j when all NLOS UEs are served by D2D relaying is formulated as the following problem.

$$\textbf{P2:} \max_{\{\mathbf{t}\}} \sum_{k=1}^{K} x_{k,j} \log \left(\sum_{q=1}^{\theta_{k,j}} \frac{C_{k,j}^{\rho_{k,j}} t_{k,j}^{\rho_{k,j},q}}{\rho_{k,j}} \right)$$
$$\text{subject to: } (7)-(9)$$

The objective function of Problem **P2** is convex and all constraints are linear. Thus, Problem **P2** a convex optimization problem, which can be optimally solved with a Lagrangian dual method.

3) Greedy Link Selection: Based on the optimal solution of problem **P2**, we develop a greedy algorithm to determine the link selection of NLOS UEs in the third stage. The idea is to iteratively evaluate the performance gain of UEs when they switch from D2D to multi-beam reflection, and select the UE(s) with the largest performance gain to make such a switching. We denote $\Delta_{k,j}^{[\tau]}$ as the performance gain of all UEs when UE k switches from D2D relaying to multi-beam reflection at the τth round of the greedy algorithm. When a UE switches to multi-beam reflection, all of its descendent UEs in the D2D tree (if there is any) would also switch to multi-beam reflection. This is because, if the descendent UEs are not switched, it is necessary to reconstruct the D2D relaying architecture, which is time-consuming. Besides, these UEs would become the descendants of other UEs, which brings a significant change of data rate to these UEs, making the evaluation of performance gain inaccurate. The performance gain of UE k and its descendent UEs when switching from D2D relaying to multi-beam reflection is calculated by: $\Delta_{k,j}^{[\tau]} = \log \tilde{R}_{k,j}^{[\tau]} - \log R_{k,j}^{[\tau]} + \sum_{k' \neq k} a_{k,k',j} \left(\log \tilde{R}_{k',j}^{[\tau]} - \log R_{k',j}^{[\tau]} \right)$.

As UEs switch from D2D relaying to multi-beam reflection, the available resources (transmission time) of D2D relaying UEs are increased, while the transmission powers of LOS UEs and multi-beam reflection UEs are decreased. For D2D relaying UEs, the values of $t_{k,j}^{\rho_{k,j},q}$ for different UEs would be close to each other under optimal resource allocation, since the objective function is the sum logarithm rate, which achieves proportional fairness. As a result, when an NLOS UE l switches from D2D relaying to multi-beam reflection, the "released" resource is approximately equally added to all the other UEs. Specifically, the values of $t_{k,j}^{\rho_{k,j},q}$ of other UEs is increased by $\frac{t_{l,j}^{\rho_{k,j},q}}{\sum_k \alpha_{k,j}}$ if UE l does not have any descendent in the D2D tree and increased by $\frac{t_{l,j}^{\rho_{l,j},q} + \sum_{l' \neq l} a_{l,l',j} t_{l',j}^{\rho_{l',j},q}}{\sum_k \alpha_{k,j}}$ if UE l has descendent(s) in the D2D tree. For UEs served by multi-beam reflection, since the BS transmission power is equally shared among them, the power allocated to each UE is decreased by a factor of $\frac{\sum_k \beta_{k,j} + N_{\mathrm{LOS},j}}{\sum_k \beta_{k,j} + 1 + N_{\mathrm{LOS},j}}$ if UE k has no descendent in the D2D tree, and decreased by $\frac{\sum_k \beta_{k,j} + N_{\mathrm{LOS},j}}{\sum_k \beta_{k,j} + 1 + \sum_{l' \neq l} a_{l,l',j} + N_{\mathrm{LOS},j}}$ otherwise.

Let Ω_j be the set of UEs served by BS j and let Φ_j be the set of UEs served by BS j via D2D relaying, $\Phi_j \subset \Omega_j$. Define the set of the descendent UEs of UE k as $\eta_{k,j} = \{k' | \, a_{k,k',j} = 1\}$. The greedy link selection scheme is summarized in Algorithm 1. In each round of Algorithm 1, the UE(s) with the largest performance gain is selected to switch from D2D relaying to multi-beam reflection. The switching process terminates until none of the UE(s) can achieve a positive performance gain, since the sum logarithm rate can not be improved when $\Delta_{k,j}^{[\tau]} \leq 0$.

Algorithm 1 Adaptive Link Selection for UEs Served by BS j

Initialize: $\alpha_{k,j} = 1, \beta_{k,j} = 0, \forall k \in \Omega_j$;
  $\Phi_j = \{k \, | \alpha_{k,j} = 1\}$;
$\tau = 1$, $l = \arg\max_{\{k \in \Phi_j\}} \Delta_{k,j}^{[1]}$;
while $\Delta_{l,j}^{[\tau]} > 0$ **do**
  if $\rho_{l,j} = 1$ **then**
    Set $\beta_{l,j} = 1$, $\alpha_{l,j} = 0$;
    Update $\Phi_j = \Phi_j - \{l\}$;
    for $k \in \Omega_j$ **do**
      Update $R_{k,j}^{[\tau]}$ with (14) by adding $t_{l,j}^{\rho_{l,j},q} / \sum_k \alpha_{k,j}$ to each $t_{k,j}^{\rho_{k,j},q}$, $k \in \Phi_j$;
      Update $\tilde{R}_{k,j}^{[\tau]}$ with (15) by multiplying $\tilde{p}_{k,j}$ with $(\sum_k \beta_{k,j} + N_{\mathrm{LOS},j}) / (\sum_k \beta_{k,j} + 1 + N_{\mathrm{LOS},j})$;
      Calculate $\Delta_{k,j}^{[\tau]}$;
    end
  else
    Set $\beta_{l,j} = 1$, $\alpha_{l,j} = 0$;
    Set $\beta_{l',j} = 1$, $\alpha_{l',j} = 0$, $\forall l' \in \eta_{l,j}$;
    Update $\Phi_j = \Phi_j - \{l\} - \eta_{l,j}$;
    for $k \in \Omega_j$ **do**
      Update $R_{k,j}^{[\tau]}$ with (14) by adding $(t_{l,j}^{\rho_{l,j},q} + \sum_{l' \neq l} a_{l,l',j} t_{l',j}^{\rho_{l',j},q}) / \sum_k \alpha_{k,j}$ to each $t_{k,j}^{\rho_{k,j},q}$, $k \in \Phi_j$;
      Update $\tilde{R}_{k,j}^{[\tau]}$ with (15) by multiplying $\tilde{p}_{k,j}$ with $(\sum_k \beta_{k,j} + N_{\mathrm{LOS},j}) / (\sum_k \beta_{k,j} + 1 + \sum_{l' \neq l} a_{l,l',j} + N_{\mathrm{LOS},j})$, $\forall k \notin \Phi_j$;
      Calculate $\Delta_{k,j}^{[\tau]}$;
    end
  end
  $l = \arg\max_{\{k \in \Phi_j\}} \Delta_{k,j}^{[\tau]}$;
  $\tau = \tau + 1$;
end

After link selection is completed, the resource allocation of UEs served by D2D links is updated by changing the objective function of Problem **P2** to $\sum_{k=1}^{K}\alpha_{k,j}\log\left(\sum_{q=1}^{\theta_{k,j}}\frac{C_{k,j}^{\rho_{k,j},q}t_{k,j}^{\rho_{k,j},q}}{\rho_{k,j}}\right)$ and solving the corresponding problem.

Lemma 1: The complexity of link selection by all BSs is $\mathcal{O}(K)$.

Proof: The time complexity of Algorithm 1 is determined by the number of UEs with $\Delta_{l,j}^{[\tau]}>0$, which is upper bounded by the number of UEs associated with BS j, i.e., $\sum_{k=1}^{K}x_{k,j}$. Considering all the j BSs, the complexity for each round of link selection is upper bounded by $\sum_{k=1}^{K}\sum_{j=1}^{J}x_{k,j}$. Thus, the total complexity of link selection based on Algorithm 1 by all BSs is $\mathcal{O}(K)$. □

Lemma 2: The value of objective function achieved by Algorithm 1 is at least $\frac{1}{\sum_{k=1}^{K}x_{k,j}}$ *of the global optimum.*

Proof: The proof is omitted for brevity. The approach is similar to the proof of Theorem 1 in our previous work [46]. □

B. Dual Decomposition-Based User Association

In this part, we present the dual decomposition-based user association. Aiming to maximize the sum logarithmic rate of all UEs, each UE needs to select the BS that provides the highest logarithmic data rate; the traffic load assigned to each BS should be properly optimized such that load balancing between BSs can be achieved. To achieve these goals, we apply dual decomposition to obtain near-optimal user association.

Let $\alpha_{k,j}(\mathbf{x})$ and $\beta_{k,j}(\mathbf{x})$ be the link selection variables obtained with the proposed link selection and resource allocation under user association $\mathbf{x}$, respectively. Similarly, we denote $R_{k,j}(\mathbf{x})$ and $\tilde{R}_{k,j}(\mathbf{x})$ as the data rates of UE k if served by BS j via D2D relaying and multi-beam reflection, respectively. Then, the user association problem is formulated as follows.

$$\begin{aligned}\textbf{P3:}\ \max_{\{\mathbf{x}\}}\ &\sum_{k=1}^{K}\sum_{j=1}^{J}x_{k,j}\left\{\alpha_{k,j}(\mathbf{x})\log R_{k,j}(\mathbf{x})\right.\\ &\left.+\beta_{k,j}(\mathbf{x})\log\tilde{R}_{k,j}(\mathbf{x})\right\}\\ \text{s.t.:}\ &\sum_{j=1}^{J}x_{k,j}\le 1,\quad k\in\mathcal{K},\qquad(24)\\ &\sum_{k=1}^{K}x_{k,j}\le U_j,\quad j\in\mathcal{J},\qquad(25)\\ &x_{k,j}\in\{0,1\},\quad k\in\mathcal{K},\ j\in\mathcal{J},\qquad(26)\end{aligned}$$

Problem **P3** is an integer programming problem, which is generally NP-hard. To derive a low-complexity solution algorithm, a dual decomposition-based approach is applied to obtain a near-optimal solution. As discussed, an important design objective of user association is achieving load balancing between BSs, which aims to find the optimal load assigned to each BS. Thus, we set the traffic loads of all BSs, denoted by $\mathbf{L}=\{L_1,\ldots,L_J\}$, as a set of auxiliary variables. Then, we add a new set of constraints, $\sum_{k=1}^{K}x_{k,j}=L_j,\ j\in\mathcal{J}$, to the problem. We also relax the integer constraint of $\{x_{k,j}\}$ be allowing them to take continuous values in $[0,1]$. With the new constraints, Problem **P3** is transformed to the following problem.

$$\begin{aligned}\textbf{P4}:\ \max_{\{\mathbf{x}\}}\ &\sum_{k=1}^{K}\sum_{j=1}^{J}x_{k,j}\left\{\alpha_{k,j}(\mathbf{x})\log R_{k,j}(\mathbf{x})\right.\\ &\left.+\beta_{k,j}(\mathbf{x})\log\tilde{R}_{k,j}(\mathbf{x})\right\}\\ \text{s.t.:}\ &(24)\text{ and }(25)\\ &\sum_{k=1}^{K}x_{k,j}=L_j,\quad j\in\mathcal{J},\qquad(27)\\ &x_{k,j}\in[0,1],\quad k\in\mathcal{K},\ j\in\mathcal{J}.\qquad(28)\end{aligned}$$

Since we aim to find the optimal BS traffic loads $\mathbf{L}$, a partial relaxation is applied on the constraints $\sum_{k=1}^{K}x_{k,j}=L_j, j\in\mathcal{J}$. Then, we have the corresponding Lagrangian function

$$\begin{aligned}&\mathcal{L}(\mathbf{x},\boldsymbol{\lambda})\\ &=\sum_{k=1}^{K}\sum_{j=1}^{J}x_{k,j}\left\{\alpha_{k,j}(\mathbf{x})\log R_{k,j}(\mathbf{x})\right.\\ &\quad\left.+\beta_{k,j}(\mathbf{x})\log\tilde{R}_{k,j}(\mathbf{x})\right\}-\sum_{j=1}^{J}\lambda_j\left(\sum_{k=1}^{K}x_{k,j}-L_j\right).\qquad(29)\end{aligned}$$

Let $g(\boldsymbol{\lambda})$ be the maximum value of $\mathcal{L}(\mathbf{x},\boldsymbol{\lambda})$ over all possible $\mathbf{x}$, given by

$$g(\boldsymbol{\lambda})=\max_{\{\mathbf{x}\}}\mathcal{L}(\mathbf{x},\boldsymbol{\lambda}).\qquad(30)$$

Then, the dual problem of **P4** is to find the $\boldsymbol{\lambda}$ that minimizes $g(\boldsymbol{\lambda})$, given by

$$\textbf{P4-Dual:}\ \min_{\{\boldsymbol{\lambda}\}}\ g(\boldsymbol{\lambda})\qquad(31)$$

where $\boldsymbol{\lambda}$ is the Lagrangian multiplier for Constraint (27).

At each iteration of the proposed dual decomposition-based solution, $\mathbf{x}$ and $\boldsymbol{\lambda}$ are iteratively updated by UEs and ENs by solving the problems given in (30) and (31), respectively.

It can be seen that the problem given in (30) (i.e., maximizing $g(\boldsymbol{\lambda})$) can be decomposed into K independent subproblems, each to be separately solved by the corresponding UE. To obtain the optimal solution of the subproblem for UE k at the t th iteration, UE k selects the optimal BS $j^{*[t]}$ according to

$$\begin{aligned}j^{*[t]}=\arg\max_{j\in\mathcal{J}}\{&\alpha_{k,j}(\mathbf{x})\log R_{k,j}(\mathbf{x})\\ &+\beta_{k,j}(\mathbf{x})\log\tilde{R}_{k,j}(\mathbf{x})-\lambda_j^{[t]}\Big\}.\qquad(32)\end{aligned}$$

In (32), $\{\alpha_{k,j}(\mathbf{x})\}$ and $\{\beta_{k,j}(\mathbf{x})\}$ are obtained via Algorithm 1 by applying $\mathbf{x}$ obtained from the previous iteration; $R_{k,j}(\mathbf{x})$ and $\log\tilde{R}_{k,j}(\mathbf{x})$ are calculated based on the obtained $\{\alpha_{k,j}(\mathbf{x})\}$ and $\{\beta_{k,j}(\mathbf{x})\}$. Once a UE completes its BS selection, it informs the selected BS by sending a notification message to the BS. Receiving the messages from the UEs, each BS j updates the user association variables related to it,

$\mathbf{x}_j = [x_{1,j}, \ldots, x_{K,j}]$, with the following

$$x_{k,j}^{[t]} = \begin{cases} 1, & j = j^{*[t]}, \\ 0, & \text{otherwise.} \end{cases} \tag{33}$$

Similarly, the problem of minimizing $g(\boldsymbol{\lambda})$ (i.e., Problem **P4-Dual**) can be decomposed into J independent subproblems, each to be solved by the corresponding BS. The subproblem to be solved BS j is given by

$$\min_{\{\boldsymbol{\lambda}\}} \; g_j(\lambda_j), \tag{34}$$

where $g_j(\lambda_j)$ is given by

$$\begin{aligned} & g_j(\lambda_j) \\ & = \max_{\{\mathbf{x}\}} \left\{ \sum_{k=1}^{K} x_{k,j} \left(\alpha_{k,j}(\mathbf{x}) \log R_{k,j}(\mathbf{x}) \right.\right. \\ & \quad \left.\left. + \beta_{k,j}(\mathbf{x}) \log \tilde{R}_{k,j}(\mathbf{x}) \right) - \lambda_j \left(\sum_{k=1}^{K} x_{k,j} - L_j \right) \right\}. \end{aligned} \tag{35}$$

BS j solves (34) with a gradient approach. At the t th iteration, BS j updates $\lambda_j^{[t]}$ by

$$\lambda_j^{[t+1]} = \lambda_j^{[t]} - s_j^{[t]} \rho_j^{[t]}, \tag{36}$$

where $\rho_j^{[t]}$ is the gradient of $g_j(\lambda_j)$ at the t th iteration, given by

$$\rho_j^{[t]} = L_j^{[t]} - \sum_{k=1}^{K} x_{k,j}^{[t]}, \tag{37}$$

and $s_j^{[t]}$ is the step size, given by

$$s_j^{[t]} = \frac{g(\boldsymbol{\lambda}^{[t]}) - g^{*[t]}}{\left\| \boldsymbol{\rho}^{[t]} \right\|^2}, \tag{38}$$

where $g^{*[t]}$ is the *estimate* for the optimal value of $g(\boldsymbol{\lambda})$ at iteration t, which is obtained by

$$g^{*[t]} = \min_{\{0 \le t' \le t\}} g(\boldsymbol{\lambda}^{[t]}) - \epsilon^{[t]}, \tag{39}$$

and $\epsilon^{[t]}$ is updated by

$$\epsilon^{[t+1]} = \begin{cases} y\epsilon^{[t]}, & \text{if } g(\boldsymbol{\lambda}^{[t+1]}) \le g(\boldsymbol{\lambda}^{[t]}), \\ \max\{z\epsilon^{[t]}, \epsilon\}, & \text{if } g(\boldsymbol{\lambda}^{[t+1]}) > g(\boldsymbol{\lambda}^{[t]}), \end{cases} \tag{40}$$

where y, z, and ϵ are predetermined positive constants with $y > 1$ and $z < 1$ [49].

With the updated $\lambda_j^{[t]}$, BS j updates its traffic load $L_j^{[t]}$ by

$$L_j^{[t+1]} = \min \left\{ \sum_{k=1}^{K} x_{k,j}^{[t]}, U_j \right\}. \tag{41}$$

Finally, BS j broadcasts the updated Lagrangian variable $\lambda_j^{[t]}$ and traffic load $L_j^{[t]}$ to nearby UEs. Based on the updated parameters, the UEs then initiate the next iteration of BS selection. The information exchange between UEs and BSs is illustrated in Fig. 4. The procedure of the dual decomposition-based user association algorithm is presented in Algorithm 2.

Algorithm 2 Dual Decomposition-Based User Association

```
Initialize L and λ ;
do
    for k = 1 : K do
        UE k selects a BS according to (32) and notifies
        the selected BS ;
    end
    for j = 1 : J do
        BS j updates x_j with (33) ;
        Updates ρ_j with (37) ;
        Updates λ_j with (36) ;
        Updates L_j with (41) ;
    end
    t++
while (x is not converged);
```

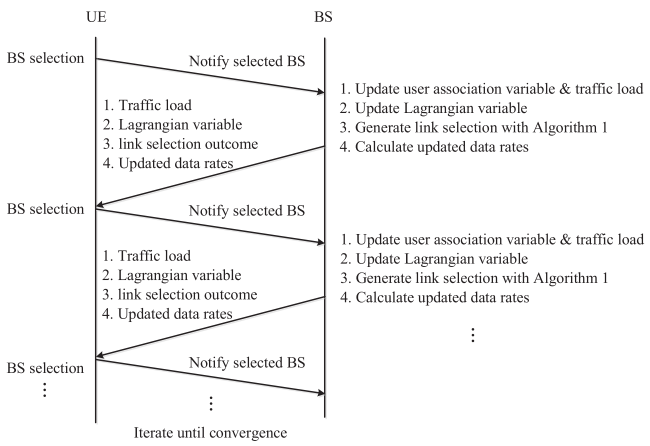

Fig. 4. Information exchange between UEs and BSs in the dual decomposition-based user association algorithm.

At each iteration of Algorithm 2, each UE makes one round of BS selection, and each BS performs one round of parameter updates. Thus, the complexity of Algorithm 2 is $Y(K + J)$, where Y is number of iterations.

Lemma 3: Algorithm 2 converges faster than the sequence $\{1/\sqrt{t}\}$.

Lemma 4: Y is upper bounded by $1/\omega^2$, where ω is the convergence threshold of $g(\boldsymbol{\lambda})$.

Proof: The proofs are omitted due to page limit, readers can refer to our previous work for more details [47]. The key idea is to analyze the optimality gap of $\boldsymbol{\lambda}$ and derive an upper bound for $\sum_{t=1}^{\infty} \left(g(\boldsymbol{\lambda}^{[t]}) - g(\boldsymbol{\lambda}^*) \right)^2$. Then, the lower bound for convergence speed of Algorithm 2 can be obtained with proof by contradiction. After Lemma 2 is proved, the number of iterations for the algorithm to achieve the optimality gap ω can be calculated. □

With Lemma 3 and Lemma 4, the complexity of the dual decomposition-based user association is $\mathcal{O}(\frac{K+J}{\omega^2})$.

Since the resource allocation given in Problem **P2** is solved with Lagrangian dual methods, the step size for updating the Lagrangian variables can be set in the same way as in (36).

Applying Lemma 4, the number of iterations for solving **P2** is upper bounded by $1/\zeta^2$, where ζ is the threshold for the convergence. As **P2** is solved by each BS in a centralized pattern, the complexity for each iteration of parameter update is $\sum_{k=1}^{K}\theta_{k,j}$, i.e., $\mathcal{O}(KN)$ [48]. Thus, the complexity of solving **P2** by all BSs is $\mathcal{O}(\frac{KNJ}{\zeta^2})$.

Based on the results above, we conclude that the complexity of the proposed solution is $\mathcal{O}(\frac{KNJ}{\zeta^2}+K+\frac{K+J}{\omega^2})$. It can be seen that solving Problem **P2** incurs the highest complexity among all the problems, while it is a standard convex optimization problem that can be efficiently solved. Thus, the proposed solution can be implemented with real-time operations.

Lemma 5: Let g^* be the optimal value of $g(\boldsymbol{\lambda})$, the optimality gap of Algorithm 2 satisfies

$$\min_{t} g(\boldsymbol{\lambda}^{[t]}) - g^* \leq \epsilon. \tag{42}$$

Proof: The derivative of $g(\boldsymbol{\lambda})$ with respect to each λ_j is given by $\frac{\partial g(\boldsymbol{\lambda})}{\partial \lambda_j} = L_j - \sum_{k=1}^{K} x_{k,j}$, which is a bounded value. According to Proposition 6.3.6 in [49], the optimality gap of $g(\boldsymbol{\lambda})$ is bounded by ϵ. □

1) Performance Bound: To demonstrate that solution obtained by the dual decomposition-based user association is near-optimal, we derive an upper bound on the performance, which will be used in simulations for comparison. As the first step, we exhaustively search all feasible vectors of $\mathbf{L}$. Under each $\mathbf{L}$, we solve the following linear programming (LP):

$$\begin{aligned}\mathbf{P5}: \max_{\{\mathbf{x}\}} & \sum_{k=1}^{K}\sum_{j=1}^{J} x_{k,j}\left\{\alpha_{k,j}(\mathbf{x})\log R_{k,j}(\mathbf{x})\right. \\ & \left.+\beta_{k,j}(\mathbf{x})\log \tilde{R}_{k,j}(\mathbf{x})\right\} \\ \text{s.t.:}\ & (24), (27) \text{ and } (28).\end{aligned}$$

Since the traffic load of each BS j ($L_j, j \in \mathcal{J}$) has U_j possible values, the total number of LPs given in **P5** is $\prod_{j=1}^{J} U_j$. Among all the $\prod_{j=1}^{J} U_j$ LPs, we select the one that generates the largest value of the objective function under optimal solution. Then, the value of the objective function of the selected LP is a performance upper bound.

V. Simulation Study

The performance of the proposed scheme is validated via MATLAB simulations. We consider a 200 m × 200 m area with varying numbers of BSs and UEs distributed in the area. The UEs can be uniformly distributed or non-uniformly distributed in the area. For the latter case, the area is divided into 8 subareas; the number of UEs in each subarea follows a Poisson distribution, and the UE densities vary across these subareas. The simulation parameters and settings are based on that in [18]; the channel model and the distance-based blockage model are also adopted from [18]. The available bandwidth is 1 GHz. The UEs are subject to random blockage and we denote $P_{k,j}^{(b)}$ as the blockage probability of UE k when associated with BS j. $P_{k,j}^{(b)}$ increases linearly with the distance between UE k and BS j with coefficient κ, given as $P_{k,j}^{(b)} = \min\{\kappa \cdot D_{k,j}, 1\}$. For example, when $\kappa = 0.05$, a UE that is 10 m away from the BS has a probability of 0.5 to be blocked; for a UE that is more than 20 m away, it is always blocked. To evaluate the effectiveness of the proposed adaptive link selection scheme, we compare it with a heuristic link selection scheme, which is performed in an iterative pattern. Specifically, in each iteration of the heuristic link selection scheme, the UE with the largest value of $\tilde{R}_{k,j}$ is selected to be served with multi-beam reflection. The iterative process terminates until $\sum_k \beta_{k,j}\tilde{R}_{k,j}$ decreases. To evaluate the effectiveness of the proposed user association scheme, we compare it with a heuristic user association scheme, in which each UE is associated with the BS that has the highest SINR. Finally, we derive a performance bound to show the optimality of the proposed scheme. Specifically, we first set the objective function of Problem **P1** to be the sum rate of all UEs, and relax the integer constraints of $\mathbf{x}$, $\boldsymbol{\alpha}$, and $\boldsymbol{\beta}$, and $\mathbf{a}$ by allowing them to take any value in $[0, 1]$. We then obtain the optimal solution of the resulting LP. The objective value under the optimal solution is an *upper bound* for the sum rate performance.

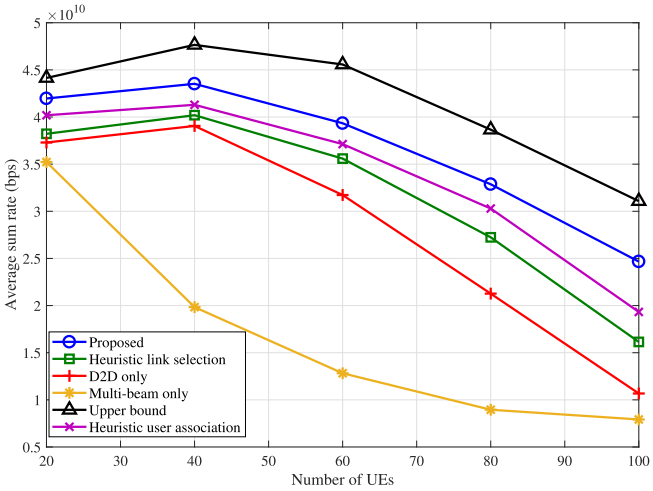

Fig. 5. Average sum rate under different numbers of UEs. Uniformly distributed UEs and $\kappa = 0.02$.

Fig. 5 shows the sum rate performance under varying numbers of UEs for the case of uniformly distributed UEs. We observe that the multi-beam only scheme achieves the worst performance among all schemes, which is caused by the high path loss and increased propagation distance of NLOS links. The D2D only scheme achieves a better performance than the multi-beam only scheme, but the data rate is significantly decreased when more UEs are served. This happens because the resource has to be shared among more UEs. By combining D2D relaying with multi-beam reflection, the heuristic link selection scheme, the heuristic user association scheme, and the proposed scheme achieve a higher sum rate, since fewer UEs are involved in D2D transmission and more resource is available for each UE. The proposed scheme outperforms the heuristic link selection scheme, because the proposed algorithm is based on evaluating the performance of UEs served by D2D and multi-beam reflection, while the heuristic link selection scheme only considers UEs served by multi-beam. It is also observed that the average data rates

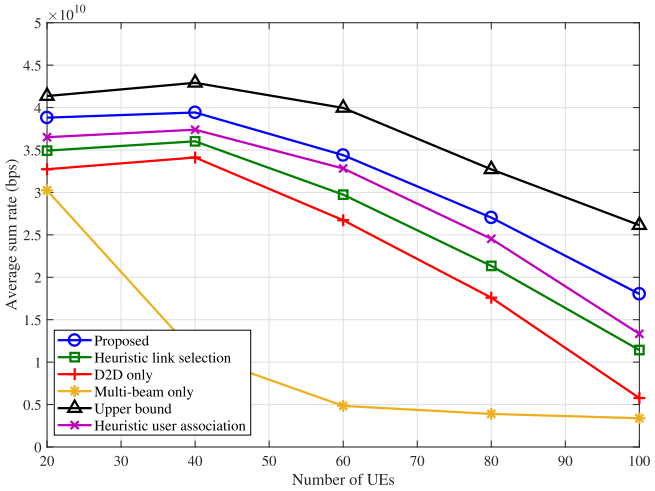

Fig. 6. Average sum rate under different numbers of UEs. Non-uniformly distributed UEs and $\kappa = 0.02$.

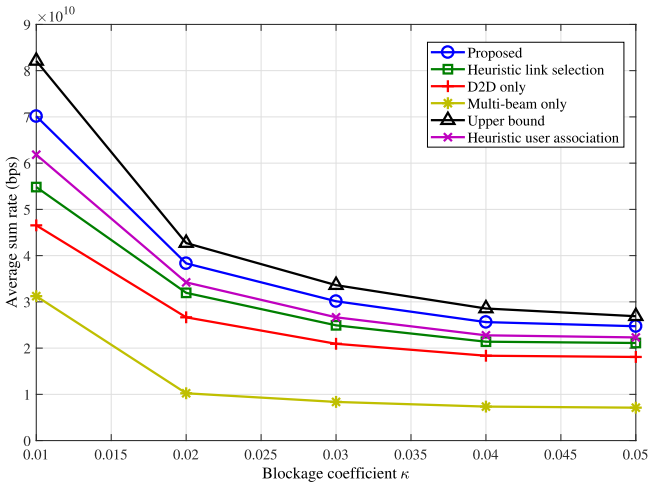

Fig. 7. Average sum rate under different values of κ. Uniformly distributed UEs and the number of UEs is 75.

of these three schemes first get higher as the number of UEs increases, since more UEs can provide relaying links to NLOS UEs. As the number of UEs continues to increase, the average data rates of these schemes are decreased, which is caused by resource sharing among UEs. The proposed scheme also outperforms the heuristic user association scheme since load balancing can be achieved via interaction between UEs and BSs, which leads to better system performance. For example, UEs in the overlapping areas of multiple BSs can handover from an overloaded BS to a less loaded BS with more communication resources. The performance achieved by the proposed scheme is close to that of the upper bound, demonstrating that the data rate performance loss caused by fairness consideration is relatively small.

Fig. 6 shows the sum rate performance under varying numbers of UEs for the cases of non-uniformly distributed UEs, where similar trends among different schemes can be observed. For the same number of UEs, the data rates of all schemes are lower compared to the case of uniformly distributed UEs. This is because the UEs are less evenly distributed among the coverage areas of BSs, making it more likely that some BSs are overloaded. It is also observed that the performance gaps between different schemes are larger compared to the case of uniformly distributed UEs, due to the fact that adaptive link selection and user association provide higher data rate improvement when the traffic load varies significantly across BSs. The results of Figs. 5 and 6 indicate that the performance of a single approach (D2D relaying only and multi-beam reflection only) is highly limited by the number of UEs. In particular, a combination of multiple approaches with proper UE selection and load balancing among BSs can significantly enhance the data rate performance.

The data rate performance versus blockage coefficients, κ, is shown in Figs. 7 and 8. As κ gets larger, the data rates of all schemes are decreased since the proportion of NLOS UEs among all UEs is increased. It can also be seen that the performance of a single approach (D2D relaying only and multi-beam reflection only) is highly sensitive to

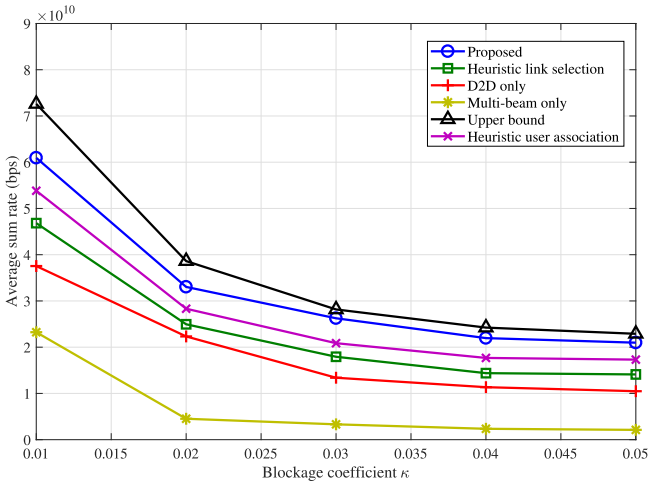

Fig. 8. Average sum rate under different values of κ. Non-uniformly distributed UEs and the number of UEs is 75.

blockage, since the time and power resources are shared by the increasing number of NLOS UEs. With adaptive link selection, the heuristic user association scheme and the proposed scheme achieve considerable performance gain compared to the single-approach schemes. Comparing Fig. 7 with Fig. 8, it can be seen that the average data rate is lower when the UEs are non-uniformly distributed, and higher performance gain can be achieved with the proposed designs.

Figs. 9 and 10 show the fairness performance of different schemes with uniformly distributed and non-uniformly distributed UEs, respectively. We use Jain's fairness index,

$$\mathcal{F} = \frac{\left(\sum_k \alpha_{k,j} R_{k,j} + \sum_k \beta_{k,j} \tilde{R}_{k,j}\right)^2}{\sum_k x_{k,j} \cdot \sum_k (\alpha_{k,j} R_k + \beta_{k,j} \tilde{R}_k)^2}$$

to measure fairness between different UEs. It can be seen that fairness is poorer for the case of non-uniformly distributed UEs. For both cases, the fairness performance is poor when the objective is set as sum rate maximization. This

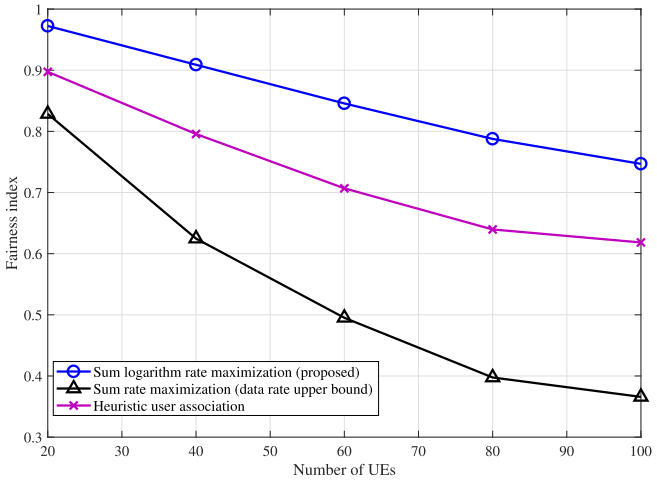

Fig. 9. Fairness of different schemes with uniformly distributed UEs. The number of UEs is 75 and $\kappa = 0.02$.

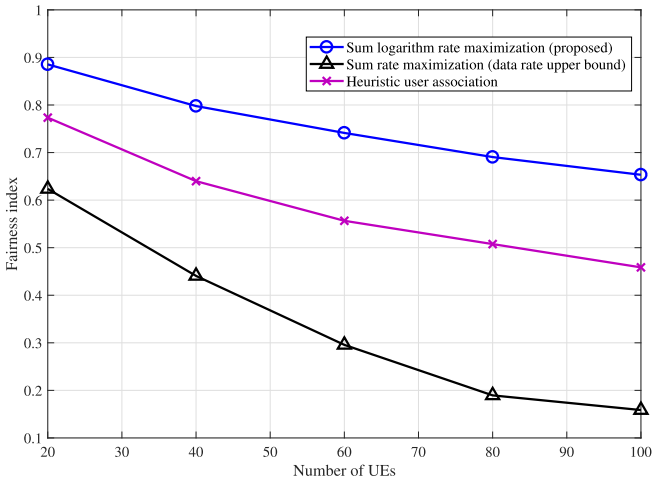

Fig. 10. Fairness of different schemes with non-uniformly distributed UEs. The number of UEs is 75 and $\kappa = 0.02$.

is because, under the optimal resource allocation, the links with better channel condition would be allocated with more communication resource than the links with worse channel condition, resulting in large variation of data rate among UEs. By setting the objective as sum logarithm rate maximization, the proposed scheme achieves a good tradeoff between sum rate performance and fairness among UEs.

VI. Conclusion

In this paper, we considered an adaptive combination of D2D relaying, multi-beam reflection, and handover to overcome blockage and improve the data rate performance of mmWave networks. We proposed a joint optimization of link selection, resource allocation, and user association and formulated it as a mixed-integer programming problem. The formulated problem was solved by decomposing it into two levels of subproblems. The lower-level subproblem is link selection and resource allocation under a given under association, which is solved by a three-stage process. The higher-level subproblem is user association, and we solved it with a dual decomposition-based approach. Simulation results indicate that the proposed scheme achieves higher data rate than several benchmark schemes, and the performance is close to an upper bound. The proposed scheme achieves a tradeoff between sum rate performance and fairness among UEs.

References

[1] M. Feng, S. Mao, and T. Jiang, "Dealing with link blockage in mmWave networks: D2D relaying or multi-beam reflection?" in *Proc. IEEE 28th Annu. Int. Symp. Pers., Indoor, Mobile Radio Commun. (PIMRC)*, Montreal, QC, Canada, Oct. 2017, pp. 1–5.

[2] Qualcomm. *The 1000X Data Challenge*. Accessed: Feb. 1, 2022. [Online]. Available: https://www.qualcomm.com/1000x

[3] J. G. Andrews *et al.*, "What will 5G be?" *IEEE J. Sel. Areas Commun.*, vol. 32, no. 6, pp. 1065–1082, Jun. 2014.

[4] T. S. Rappaport *et al.*, "Millimeter wave mobile communications for 5G cellular: It will work!" *IEEE Access*, vol. 1, pp. 335–349, 2013.

[5] Z. He and S. Mao, "A decomposition principle for link and relay selection in dual-hop 60 GHz networks," in *Proc. IEEE 35th Annu. IEEE Int. Conf. Comput. Commun. (INFOCOM)*, San Francisco, CA, USA, Apr. 2016, pp. 1683–1691.

[6] M. Alrabeiah and A. Alkhateeb, "Deep learning for mmWave beam and blockage prediction using sub-6 GHz channels," *IEEE Trans. Commun.*, vol. 68, no. 9, pp. 5504–5518, Sep. 2020.

[7] Z. He, S. Mao, S. Kompella, and A. Swami, "On link scheduling in dual-hop 60-GHz mmwave networks," *IEEE Trans. Veh. Technol.*, vol. 66, no. 12, pp. 11180–11192, Dec. 2017.

[8] J. Qiao, X. Shen, J. Mark, Q. Shen, Y. He, and L. Lei, "Enabling device-to-device communications in millimeter-wave 5G cellular networks," *IEEE Commun. Mag.*, vol. 53, no. 1, pp. 209–215, Jan. 2015.

[9] S. Wu, R. Atat, N. Mastronarde, and L. Liu, "Improving the coverage and spectral efficiency of millimeter-wave cellular networks using device-to-device relays," *IEEE Trans. Commun.*, vol. 66, no. 5, pp. 2251–2265, May 2018.

[10] H. Zhang, S. Chong, X. Zhang, and N. Lin, "A deep reinforcement learning based D2D relay selection and power level allocation in mmWave vehicular networks," *IEEE Wireless Commun. Lett.*, vol. 9, no. 3, pp. 416–419, Mar. 2020.

[11] Y. Niu, Y. Liu, Y. Li, X. Chen, Z. Zhong, and Z. Han, "Device-to-device communications enabled energy efficient multicast scheduling in mmWave small cells," *IEEE Trans. Commun.*, vol. 66, no. 3, pp. 1093–1109, Mar. 2018.

[12] Y. Niu, C. Gao, Y. Li, L. Su, D. Jin, and A. V. Vasilakos, "Exploiting device-to-device communications in joint scheduling of access and backhaul for mmWave small cells," *IEEE J. Sel. Areas Commun.*, vol. 33, no. 10, pp. 2052–2069, May 2015.

[13] Q. Xue, X. Fang, and C.-X. Wang, "Beamspace SU-MIMO for future millimeter wave wireless communications," *IEEE J. Sel. Areas Commun.*, vol. 35, no. 7, pp. 1564–1575, Jul. 2017.

[14] S.-C. Lin and I. F. Akyildiz, "Dynamic base station formation for solving NLOS problem in 5G millimeter-wave communication," in *Proc. IEEE Conf. Comput. Commun. (INFOCOM)*, Atlanta, GA, USA, May 2017, pp. 1–9.

[15] A. Alkhateeb, I. Beltagy, and S. Alex, "Machine learning for reliable mmWave systems: Blockage prediction and proactive handoff," in *Proc. IEEE Global Conf. Signal Inf. Process. (GlobalSIP)*, Anaheim, CA, USA, Nov. 2018, pp. 1055–1059.

[16] L. Sun, J. Hou, and T. Shu, "Spatial and temporal contextual multi-armed bandit handovers in ultra-dense mmWave cellular networks," *IEEE Trans. Mobile Comput.*, vol. 20, no. 12, pp. 3423–3438, Dec. 2021.

[17] Y. Wang, S. Mao, and T. S. Rappaport, "On directional neighbor discovery in mmWave networks," in *Proc. IEEE 37th Int. Conf. Distrib. Comput. Syst. (ICDCS)*, Atlanta, GA, USA, Jun. 2017, pp. 1704–1713.

[18] J. G. Andrews *et al.*, "Modeling and analyzing millimeter wave cellular systems," *IEEE Trans. Commun.*, vol. 65, no. 1, pp. 403–430, Jan. 2017.

[19] M. R. Akdeniz *et al.*, "Millimeter wave channel modeling and cellular capacity evaluation," *IEEE J. Sel. Areas Commun.*, vol. 32, no. 6, pp. 1164–1179, Jun. 2014.

[20] R. W. Heath, N. González-Prelcic, S. Rangan, W. Roh, and A. M. Sayeed, "An overview of signal processing techniques for millimeter wave MIMO systems," *IEEE J. Sel. Topics Signal Process.*, vol. 10, no. 3, pp. 436–453, Apr. 2016.

[21] H. Shokri-Ghadikolaei *et al.*, "Millimeter wave cellular networks: A MAC layer perspective," *IEEE Trans. Commun.*, vol. 63, no. 10, pp. 3437–3458, Oct. 2015.
[22] Y. Chen, D. Chen, Y. Tian, and T. Jiang, "Spatial lobes division based low complexity hybrid precoding and diversity combining for mmWave IoT systems," *IEEE Internet Things J.*, vol. 6, no. 2, pp. 3228–3239, Apr. 2019.
[23] A. Alkhateeb, G. Leus, and R. W. Heath, "Limited feedback hybrid precoding for multi-user millimeter wave systems," *IEEE Trans. Wireless Commun.*, vol. 14, no. 11, pp. 6481–6494, Nov. 2015.
[24] C. N. Barati *et al.*, "Initial access in millimeter wave cellular systems," *IEEE Trans. Wireless Commun.*, vol. 15, no. 12, pp. 7926–7940, Dec. 2016.
[25] M. Giordani, M. Polese, A. Roy, D. Castor, and M. Zorzi, "A tutorial on beam management for 3GPP NR at mmWave frequencies," *IEEE Commun. Surveys Tuts.*, vol. 21, no. 1, pp. 173–196, 1st Quart., 2019.
[26] M. Feng, B. Akgun, I. Aykin, and M. Krunz, "Beamwidth optimization for 5G NR millimeter wave cellular networks: A multi-armed bandit approach," in *Proc. IEEE Int. Conf. Commun. (ICC)*, Jun. 2021, pp. 1–6.
[27] J. Qiao, L. X. Cai, X. S. Shen, and J. W. Mark, "Enabling multi-hop concurrent transmissions in 60 GHz wireless personal area networks," *IEEE Trans. Wireless Commun.*, vol. 10, no. 11, pp. 3824–3833, Nov. 2011.
[28] D. Moltchanov, R. Kovalchukov, M. Gerasimenko, S. Andreev, Y. Koucheryavy, and M. Gerla, "Socially inspired relaying and proactive mode selection in mmWave vehicular communications," *IEEE Internet Things J.*, vol. 6, no. 3, pp. 5172–5183, Jun. 2019.
[29] Z. Li, L. Xiang, X. Ge, G. Mao, and H.-C. Chao, "Latency and reliability of mmWave multi-hop V2 V communications under relay selections," *IEEE Trans. Veh. Technol.*, vol. 69, no. 9, pp. 9807–9821, Sep. 2020.
[30] C. G. Ruiz, A. P.-Iserte, and O. Muñoz, "Analysis of blocking in mmWave cellular systems: Application to relay positioning," *IEEE Trans. Commun.*, vol. 69, no. 2, pp. 1329–1342, Feb. 2021.
[31] Y. Niu *et al.*, "Relay-assisted and QoS aware scheduling to overcome blockage in mmWave backhaul networks," *IEEE Trans. Veh. Technol.*, vol. 68, no. 2, pp. 1733–1744, Feb. 2019.
[32] W. Khawaja, O. Ozdemir, Y. Yapici, F. Erden, and I. Guvenc, "Coverage enhancement for NLOS mmWave links using passive reflectors," *IEEE Open J. Commun. Soc.*, vol. 1, pp. 263–281, 2020.
[33] L. Zhang, X. Chen, Y. Fang, X. Huang, and X. Fang, "Learning-based mmWave V2I environment augmentation through tunable reflectors," in *Proc. IEEE Global Commun. Conf. (GLOBECOM)*, Waikoloa, HI, USA, Dec. 2019, pp. 1–6.
[34] C. K. Anjinappa, F. Erden, and I. Guvenc, "Base station and passive reflectors placement for urban mmWave networks," *IEEE Trans. Veh. Technol.*, vol. 70, no. 4, pp. 3525–3539, Apr. 2021.
[35] X. Hu, T. Liu, and T. Shu, "Fast and high-resolution NLoS beam switching over commercial off-the-shelf mmWave devices," *IEEE Trans. Mobile Comput.*, early access, Mar. 9, 2021, doi: 10.1109/TMC.2021.3064809.
[36] P. Wang, J. Fang, L. Dai, and H. Li, "Joint transceiver and large intelligent surface design for massive MIMO mmWave systems," *IEEE Trans. Wireless Commun.*, vol. 20, no. 2, pp. 1052–1064, Feb. 2021.
[37] L. Yan *et al.*, "Machine learning-based handovers for sub-6 GHz and mmWave integrated vehicular networks," *IEEE Trans. Wireless Commun.*, vol. 18, no. 10, pp. 4873–4885, Oct. 2019.
[38] L. Sun, J. Hou, and T. Shu, "Optimal handover policy for mmWave cellular networks: A multi-armed bandit approach," in *Proc. IEEE Global Commun. Conf. (GLOBECOM)*, Waikoloa, HI, USA, Dec. 2019, pp. 1–6.
[39] L. Jiao, P. Wang, A. Alipour-Fanid, H. Zeng, and K. Zeng, "Enabling efficient blockage-aware handover in RIS-assisted mmWave cellular networks," *IEEE Trans. Wireless Commun.*, early access, Sep. 15, 2021, doi: 10.1109/TWC.2021.3110522.
[40] A. Mesodiakaki, F. Adelantado, L. Alonso, M. Di Renzo, and C. Verikoukis, "Energy- and spectrum-efficient user association in millimeter-wave backhaul small-cell networks," *IEEE Trans. Veh. Technol.*, vol. 66, no. 2, pp. 1810–1821, Feb. 2017.
[41] A. Alizadeh and M. Vu, "Load balancing user association in millimeter wave MIMO networks," *IEEE Trans. Wireless Commun.*, vol. 18, no. 6, pp. 2932–2945, Jun. 2019.
[42] M. Sana, A. De Domenico, W. Yu, Y. Lostanlen, and E. Calvanese Strinati, "Multi-agent reinforcement learning for adaptive user association in dynamic mmWave networks," *IEEE Trans. Wireless Commun.*, vol. 19, no. 10, pp. 6520–6534, Oct. 2020.
[43] R. Liu, Q. Chen, G. Yu, and G. Y. Li, "Joint user association and resource allocation for multi-band millimeter-wave heterogeneous networks," *IEEE Trans. Commun.*, vol. 67, no. 12, pp. 8502–8516, Dec. 2019.
[44] Z. He, S. Mao, and T. S. Rappaport, "On link scheduling under blockage and interference in 60-GHz ad hoc networks," *IEEE Access*, vol. 3, pp. 1437–1449, 2015.
[45] Z. Xiao, H. Wen, A. Markham, N. Trigoni, P. Blunsom, and J. Frolik, "Non-line-of-sight identification and mitigation using received signal strength," *IEEE Trans. Wireless Commun.*, vol. 14, no. 3, pp. 1689–1702, Mar. 2015.
[46] M. Feng, S. Mao, and T. Jiang, "Joint duplex mode selection, channel allocation, and power control for full-duplex cognitive femtocell networks," *Digit. Commun. Netw.*, vol. 1, no. 1, pp. 30–44, Feb. 2015.
[47] M. Feng, S. Mao, and T. Jiang, "Joint frame design, resource allocation and user association for massive MIMO heterogeneous networks with wireless Backhaul," *IEEE Trans. Wireless Commun.*, vol. 17, no. 3, pp. 1937–1950, Mar. 2018.
[48] Q. Ye, B. Rong, Y. Chen, M. Al-Shalash, C. Caramanis, and J. G. Andrews, "User association for load balancing in heterogeneous cellular networks," *IEEE Trans. Wireless Commun.*, vol. 12, no. 6, pp. 2706–2716, Jun. 2013.
[49] D. Bertsekas, *Convex Optimization Theory*. Belmont, MA, USA: Athena Scientific, 2009.